UC San Diego
UC San Diego Previously Published Works

Title

Photothermal immunotherapy of melanoma using TLR-7 agonist laden tobacco mosaic virus with polydopamine coat.

Permalink

https://escholarship.org/uc/item/8c85g259

Authors

Nkanga, Christian
Ortega-Rivera, Oscar
Steinmetz, Nicole

Publication Date

2022-08-01

DOI

10.1016/j.nano.2022.102573

Peer reviewed

Photothermal immunotherapy of melanoma using TLR-7 agonist laden tobacco mosaic virus with polydopamine coat

Christian Isalomboto Nkanga, PhD[a], **Oscar A. Ortega-Rivera, PhD**[a,d], **Nicole F. Steinmetz, PhD**[a,b,c,e,f,*]

[a]Department of NanoEngineering, University of California San Diego, 9500 Gilman Dr., La Jolla, CA 92039, United States

[b]Department of Bioengineering, University of California San Diego, 9500 Gilman Dr., La Jolla, CA 92039, United States

[c]Department of Radiology, University of California San Diego, 9500 Gilman Dr., La Jolla, CA 92039, United States

[d]Center for Nano-ImmunoEngineering, University of California San Diego, 9500 Gilman Dr., La Jolla, CA 92039, United States

[e]Moores Cancer Center, University of California San Diego, 9500 Gilman Dr., La Jolla, CA 92039, United States

[f]Institute for Materials Discovery and Design, University of California San Diego, 9500 Gilman Dr., La Jolla, CA 92039, United States

Abstract

Photothermal therapy (PTT) is a promising cancer treatment that debulks tumors locally while priming immune responses. However, PTT as a standalone treatment approach often has limited systemic efficacy, motivating the development of synergistic combination approaches. Toward this goal, herein, the tobacco mosaic virus (TMV) was loaded with a small molecule immunomodulator, toll-like receptor 7 agonist (1V209), and its surface was coated with photothermal biopolymer polydopamine (PDA). The resulting 1V209-laden and PDA-coated TMV was used to treat B16F10 dermal melanoma in C57BL/6 mice. 1V209-TMV-PDA was intratumorally injected and irradiated using an 808-nm near infrared laser. 60 % of the mice receiving PTT with intratumoral 1V209-TMV-PDA + laser remained alive at the end point

*Corresponding author at: Department of NanoEngineering, University of California San Diego, 9500 Gilman Dr., La Jolla, CA 92039, United States. nsteinmetz@ucsd.edu (N.F. Steinmetz).

– in contrast to only 20 % survivors were observed in the control group. Immunological analysis indicates systemic anti-tumor immunity being induced by the combination therapy with a greater number of tumor-specific T cells (as determined by a splenocyte assay). This study highlights the potential of TMV versatility as a multifunctional nano-platform for combined PTT-immunotherapy.

Keywords

Photothermal therapy; Anti-tumor immunotherapy; TLR-7 agonist; Melanoma; Nanoparticles; Polydopamine; Tobacco mosaic virus

Background

Melanoma is one of the most clinically relevant skin and soft tissue malignancies. While it only counts for about 1 % of skin cancers,[1] melanoma causes up to 65 % of skin cancer-related deaths, with only 5 % of long-term survival rate.[2] In situ tumor ablation strategies such as surgical excision and radiotherapy have shown some success by debulking localized disease; however, tumor recurrence in the same or distant site of the original melanoma remains a major challenge in oncology.[3] Photothermal therapy (PTT) is another promising non-invasive tumor ablation treatment that debulks accessible cancerous tissues while simultaneously activating the immune system against metastasis or tumor recurrence.[4] PTT reagents efficiently convert light from a near infrared laser into heat that causes immunogenic cancer cell death, priming antitumor immune responses through damage-associated molecular patterns.[5,6] Gold nanoparticles make excellent PTT agents; and it has been shown that PTT with intratumoral gold nanoparticles elicits pro-inflammatory cytokines and chemokines, therefore inducing dendritic cell maturation and antigen processing – processes that ultimately trigger anti-tumor T cell responses.[7] Many other nanomaterials (incl. Carbon nanotubes) have been used for PTT owing to their abilities to act as photosensitizers or photothermal transducers.[8] Nonetheless, several studies showed that PTT-induced anti-tumor immunity is insufficient to circumvent melanoma recurrence (or metastasis) on its own, requiring additional immunotherapeutic interventions such as the use of adoptive T cell transfer[7] or immunostimulatory adjuvants such as CpG-containing oligodeoxynucleotides[9] or immunomodulatory virus-like particles (VLPs).[10]

VLPs or their infectious counterparts – the plant virus nanoparticles (VNPs), make attractive platforms for PTT approaches. The VLP or VNP itself could prime anti-tumor immunity through recognition of pattern recognition receptors (PRRs).[11,12] Further positive attributes of the VLP/VNP platform technology are: high degree of biocompatibility, ease of large-scale manufacture through fermentation or molecular farming, as well as the highly defined, multivalent nanoparticle platforms that can be functionalized with cargo.[13–15] For example, in a recent study VLPs derived from bacteriophage $Q\beta$ were decorated with croconium, a near-infrared dye, to produce a photothermal phage that effectively ablated primary breast tumors and reduced lung metastasis in tumor mouse models.[10] In this work, we turned toward the high aspect ratio, hollow nanotubes formed by the tobacco mosaic virus (TMV). TMV is a highly robust platform nanotechnology – the nanotubes are composed of 2130

identical coat protein units forming a 300×18 nm nucleocapsid with a 4 nm channel, trapping a single-stranded RNA. TMV particles can withstand multiple rounds of chemical modifications on both, the interior and exterior surface.[16–19] Toward PTT strategies, we developed methods to coat TMV with the biopolymer polydopamine (PDA).[20,21] PDA is a melanin-like biopolymer widely used as a coating agent[9,22] or drug delivery matrix[23,24] for photothermal immunotherapy owing to its excellent photothermal conversion efficiency. And indeed, our previous study demonstrated that PDA-coated TMV (TMV-PDA) conferred photothermal and photoacoustic properties.[20,21]

In this work, we set out to test the anti-tumor efficacy of TMV-PDA. We previously reported moderate immunomodulatory properties of TMV alone,[25] therefore we equipped TMV with an additional immunodulator, specifically the small molecule 1V209 (2-methoxyethoxy-8-oxo9-(4-carboxy benzyl) adenine), which is a toll-like receptor (TLR)-7 agonist. TLR7 ligands are established immune enhancers acting through co-activation of various immune cells, cytokines, and chemokines, and have been used to mount systemic anti-tumor immunity and immune memory.[26,27] 1V209 is a synthetic nucleoside-like TLR7 agonist reported to be active against both primary tumor and metastatic stages of various malignancies, including melanoma[28] and breast cancer.[29] However, like other small molecules, 1V209 has poor pharmacokinetics and rapid wash-out effects in the tumor that require a delivery system (via nanoparticles or polymers) to improve its solubility and tumor residence time.[30,31] TMV therefore could act as the 1V209 delivery system while serving as an immunomodulator and PTT agent when also coated with PDA. We developed the 1V209-TMV-PDA formulation and tested the efficacy of the combination of PTT approach using a mouse model of dermal melanoma (B16F10 cells and C57BL/6 mice).

Methods

Particles production and evaluation

TMV propagation and purification—TMV was extracted from infected leaves of *Nicotiana benthamiana* using established protocols.[32] In short, frozen leaves were homogenized in aqueous mixture of 0.1 M potassium phosphate (KP) buffer and 0.2 % (v/v) 2-mercaptoethanol (Thermo Fisher Scientific). The homogenate was filtered through 2 layers of cheesecloth, and the filtrate was centrifuged (11,000 ×g, 4 °C, 20 min) to remove plant material. The supernatant was extracted with 1:1 (v/v) mixture of chloroform: butanol-1; the aqueous phase was decanted and stirred at 4 °C overnight with 0.2 M NaCl and 8 % (w/v) polyethylene glycol (PEG) 8000 (Thermo Fisher Scientific) to precipitate TMV particles. The precipitate was pelleted (22,000 ×g, 20 min, 4 °C), redispersed in 0.01 M KP buffer and the resultant suspension was further centrifuged (15,000 ×g, 15 min, 4 °C) to remove polymer aggregates. The resultant supernatant was centrifuged over a 40 % (w/v) sucrose cushion (160,000 ×g, 4 °C, 3 h) to pellet TMV. The isolated TMV particles were dispersed in 0.01 M KP buffer, and the concentration was measured by UV spectrometry using a NanoDrop 2000 spectrophotometer (Thermo Fisher Scientific) at 260 nm, with a molar extinction coefficient ($\varepsilon_{260\ nm}$) of 3.0 mg^{-1} mL cm^{-1}.

Conjugation of 1V209 to TMV—1V209-loaded TMV particles (1V209-TMV) were prepared using a two-step protocol: first, TMV and 1V209 were separately modified through alkyne and azide labeling, respectively; then, the resultant derivatives were conjugated by copper-catalyzed azide–alkyne cycloaddition (click chemistry). *Alkyne labeling of TMV*: A mixture of 2 mL 10 mg mL^{-1} TMV (in 0.01 M KP buffer), 5.74 mL 0.1 M HEPES (pH 7.4), 1.3 mL 0.1 M propargylamine and 30 mg hydroxybenzotriazole (HOBt; Sigma-Aldrich) was briefly vortexed, and three portions of 0.32 mL 0.1 M *N*-(3-dimethylaminopropyl)-*N*´-ethyl carbodiimide (EDC, Sigma-Aldrich) were subsequently added at room temperature under stirring at time = 0, 6 and 18 h. After all EDC additions, the reaction medium was further stirred for 24 h. TMV particles labeled with alkyne handles (alkyne-TMV) were isolated by ultracentrifugation (160,000 ×g, 4 °C, 3 h) over a 40 % (w/v) sucrose cushion. *Azide-labeling of 1V209*: 0.1 mL of 0.025 M aminooxy-PEG1-azide (Broadpharm) in DMSO was added to a mixture of 0.1 mL 0.1 M 1V209 (MedChemExpress) in DMSO, 30 mg HOBt (Sigma-Aldrich), 1.8 mL fresh DMSO and 1 mL of 0.1 M HEPES (pH 7.4). Then, 0.33 mL of 0.1 M EDC was added after 0, 6 and 18 h of stirring at room temperature. The resultant mixture was stirred for another 24 h and then centrifuged at 7500 ×g for 5 min at room temperature to remove any 1V209 precipitates, keeping soluble azide-labeled 1V209 (azide-1V209) in solution. *Click chemistry*: The supernatant containing the azide-1V209 was transferred to 16 mL of 1.1 mg mL^{-1} alkyne-TMV in 0.01 M KP buffer at 4 °C; and the following reagents were added:[33] 0.1 mL of 0.2 M aminoguanidine, 0.1 mL of 0.2 M sodium ascorbate and 0.1 mL of 0.1 M CuSO$_4$ (Acros Organics). The obtained mixture was stirred for 30 min at 4 °C; to stop the reaction, 0.1 mL of 0.5 M EDTA (Sigma-Aldrich) was added over 5 min at room temperature. The prepared 1V209-TMV particles were pelleted over a 40 % (w/v) sucrose cushion (133,000 ×g, 4 °C, 1 h), resuspended in 0.01 M KP, and characterized by UV spectrometry, sodium dodecylsulfate polyacrylamide gel electrophoresis (SDS-PAGE), liquid chromatography mass spectrometry (LC-MS) and transmission electron microscopy (TEM) (as described below).

Coating of 1V209-TMV with polydopamine—Polydopamine coat was added to 1V209-TMV using in situ oxidative polymerization of dopamine as previously reported.[20] Briefly, we stirred 12 mg of dopamine (Sigma-Aldrich) with 8 mg of 1V209-TMV in 80 mL of Tris buffer (pH 8.5) at room temperature for 6 h. The reaction medium was centrifuged (25,000 ×g, 4 °C, 20 min), and the pelleted particles were washed first with phosphate-buffered saline (PBS) and after with Millipore water. Native TMV particles were coated using the same protocol to prepare TMV-PDA as well as blank PDA. Polydopamine-coated particles were characterized by TEM and photothermal analysis.

1V209-TMV-PDA characterization

Sodium dodecylsulfate polyacrylamide gel electrophoresis (SDS-PAGE)—TMV samples were mixed with loading buffer (made up of 62.5 mM Tris–HCl pH 6.8, 2 % (w/v) SDS, 10 % (v/v) glycerol, 0.01 % (w/v) bromophenol blue, 10 % (v/v) 2-mercaptoethanol) and denatured at 100 °C for 5 min; coat proteins (CPs) were separated on 4–12 % or 12 % NuPAGE polyacrylamide gels using in 1× (3-(N-morpholino) propanesulfonic acid) buffer (MOPS, Invitrogen) at 200 V and 120 mA for 40 min. SeeBlue Plus2 pre-stained protein

standards (Thermo Fisher Scientific) was used as a molecular weight ladder. Gels were imaged using ProteinSimple FluorChem R imaging system.

Liquid chromatography mass spectrometry (LC-MS)—To verify successful conjugation of 1V209 to TMV, 1V209-TMV or TMV were disassembled into individual CP units prior to LC-MS analysis. To disassemble TMV into CPs, 0.2 mL of 10 mg mL^{-1} samples was added to 0.4 mL of glacial acetic acid and the resultant mixture was incubated on ice for 20 min prior to vortexing and centrifugation (20,000 xg, 20 min, 4 °C) to pellet the RNA. The resultant supernatant was transferred to 6–8 MWCO dialysis tubing (Spectra/Por) and dialyzed against 2 L of di-ionized water at 4 °C for 48 h, with one water change after 24 h. After dialysis, a white precipitate was observed in the tubing and the pH of the dialysis liquid was 4.4. The observed white precipitate (CPs) was pelleted by spinning (20,000 xg, 4 °C, 20 min) and redissolved in 0.4 mL of 0.01 M KP. The obtained CP solution was analysed using an Agilent 6230 time-of-flight mass spectrometer (TOFMS) with Jet Stream electrospray ionization source (ESI). The Jet Stream ESI source was operated under positive ion mode with the following parameters: VCap = 3500 V, fragmentor voltage = 175 V, drying gas temperature = 325 °C, sheath gas temperature = 325 °C, drying gas flow rate = 10 L min^{-1}, sheath gas flow rate = 10 L min^{-1}, nebulizer pressure = 40 psi. The chromatographic separation was performed at room temperature on a Phenomenex Aeries Wide pore XB-C18 column (2.1 mm ID × 50 mm length, 3.6 μm particle size). Mobile phase A was HPLC grade water with 0.1 % (v/v) trifluoroacetic acid (TFA), and HPLC grade acetonitrile with 0.1 % (v/v) TFA was used as mobile phase B. The mobile phase was delivered at a rate of 0.3 mL min^{-1} under gradient conditions as followed: Increased from 5 % mobile phase B to 90 % mobile phase B in 12 min, held at 90 % mobile phase B for 2 min, returned to 5 % mobile phase B in 1 min, and equilibrated with 5 % mobile phase B for 7 min. Agilent Mass Hunter software was used for data acquisition and analysis. Based on calculated molecular weights and native TMV CPs (reference sample), the mass peak of each molecular species (1V209-conjugated CP and unreacted CP) was assigned, and mass-to-charge ratios were used to locate their corresponding elution peaks on the chromatogram. The peak areas for both 1V209-conjugated CP and unreacted CP were measured, and data was used to determine the loading of 1V209 on TMV.

Transmission electron microscopy (TEM)—1V209-TMV-PDA samples and controls (0.5 mg mL^{-1}) were deposited on carbon-coated copper grids; excess liquid was removed with filter paper and the grid was rinsed with deionized water and stained with 2 % (w/v) uranyl acetate. TMV particles were visualized under a FEI Tecnai Spirit G2 BioTWIN TEM (at 80 kV).

Photothermal measurements—1V209-TMV-PDA samples and controls (1 mL) containing different concentrations (0–0.3 mg mL^{-1}) of 1V209-TMV-PDA particles were irradiated with an 808 nm laser (near-infrared laser MDL-808–2 W, Changchun New Industries Tech. Co., Ltd.) in a quartz cuvette with a power setting of 1 W cm^{-2} for 10 min. The change in temperature was monitored by means of an A300 forward-looking infrared (FLIR) thermal camera (Mid-State Instruments LLC).

RAW-Blue™ cell assay—RAW-Blue cells (Invivogen) are derived from the murine RAW 264.7 macrophages with chromosomal integration of a secreted embryonic alkaline phosphatase (SEAP) reporter construct inducible by NF-κB and AP-1. RAW-Blue cells express pattern-recognition receptors (PRRs), including toll-like receptors (TLRs), NOD-like receptors (NLRs), RIG-I-like receptors (RLRs) and C-type lectin receptors (CLRs). RAW-Blue cells were cultured in Dulbecco's modified Eagle's medium (DMEM, from Corning Life Sciences) supplemented with 10 % (v/v) heat-inactivated Fetal bovine serum (FBS) from Atlanta Biologicals. Cells (10^5 in 180 μL DMEM per well) were placed on 96-well tissue plate and particles (1 μg in 20 μL) were added to the wells. After incubating for 20 h, the supernatant (20 μL per well) was transferred to another 96-well plate and QUANTI-Blue™ solution (180 μL per well) was added. The resultant mixture was incubated at 37 °C in a 5 % CO_2 atmosphere for 5 h prior to determination of the SEAP levels using a microplate reader (Tecan) at 655 nm.

Animal experiments

Ethical statements—All mouse studies were performed in compliance with the Institutional Animal Care and Use Committee (IACUC) of the University of California San Diego (UCSD) following the procedures approved by the UCSD Animal Ethics committee. We used C57BL/6 male mice (strain #000664, 7–8 weeks old) that were purchased from The Jackson Laboratory and housed at the UCSD Moores Cancer Center with full access to food and water.

Cancer cell culture—B16F10 and NIH3T3 cells (ATCC) were cultured in DMEM (Corning Life Sciences) supplemented with 10 % (v/v) fetal bovine serum + antibiotics (1 % (v/v) penicillin/streptomycin). CT26 cells (ATCC) were grown in ATCC-formulated RPMI 1640 medium supplemented with 10 % (v/v) fetal bovine serum (Atlanta Biologicals) and 1 % (v/v) penicillin/streptomycin (Thermo Fisher Scientific). All tissue culture flasks were maintained at 37 °C in a 5 % CO_2 chamber.

Tumor challenge and photothermal treatments—C57BL/6 male mice were intradermally injected with B16F10 cells (5×10^5 cells, 50 μL PBS per mouse) into the shaved right flank. Eight-to-ten days following tumor cell inoculation, when tumor volumes reached up to 100 mm³, mice were randomized into 5 groups for the following intratumoral (I.T.) treatments: (i) 100 μL PBS (n = 10); (ii) 200 μg 1V209-TMV in 100 μL PBS (n = 9); (iii) 200 μg 1V209-TMV-PDA in 100 μL PBS (n = 8); (iv) 200 μg 1V209-TMV-PDA in 100 μL PBS + laser irradiation (n = 9); and (v) laser irradiation (n = 10). Laser irradiation was performed 2 h or 1 day after respective I.T. injections, and the 808 nm NIR laser MDL-808–2 W was used to irradiate the tumor site at power of 1 W cm⁻² for 5 min. The variation in local temperature at the surface of the tumor site was recorded using the A300 FLIR thermal camera. Disease burden was monitored by measuring tumor volume, body weight and surviving mice were numbered every 2–3 days. Tumor sizes were measured by means of callipers and the volumes were calculated using to the following formula:

$$\text{Tumor volume } (\text{mm}^3) = (\text{tumor length}) \times (\text{tumor width})^2/2 .$$

Enzyme-linked immunospot (ELISpot) assay—Fifty days post tumor inoculation, surviving mice (5/9 from group 1V209-TMV-PDA + laser irradiation and 2/10 from group laser irradiation) were sacrificed and their spleens harvested for ELISpot analysis of their splenocytes; two healthy age-matched C57BL/6 mice (14–16 weeks old) were used as naïve controls. We coated the 96-well ELISpot plates (Cellular Technology Limited) with a 1:166 dilution of the anti-mouse interferon gamma (IFN-γ) capture antibody overnight at 4 °C. The splenocyte suspension was isolated from each mouse following spleen dissociation kit manufacturer directions (Miltenyi Biotec). The splenocytes from each group were seeded to the plates (5×10^5 cells per well in 100 μL) following stimulation with 100 μL of the medium alone (negative control), 1V209-TMV (10 μg/well), a mix of 50 ng/mL phorbol 12-myristate 13-acetate (PMA) and 1 μM ionomycin (Sigma-Aldrich) (positive control), B16F10 cells (5×10^5 cells per well in 100 μL), NIH3T3 cells (5×10^5 cells per well in 100 μL), or CT26 cells (5×10^5 cells per well in 100 μL) at 37 °C and 5 % CO_2 for 36 h. All cells and stimulants were prepared in FBS-free media (Cellular Technology Limited). After incubation, the plates were washed with PBST and then incubated with a 1:1000 dilution of FITC-labeled anti-mouse IFN-γ at room temperature for 2 h. The plates were then washed with PBST and incubated at room temperature for 1 h with anti-FITC-HRP secondary antibodies (diluted 1:1000). Plates were washed with PBST and distilled water, then incubated with the HRP substrate for 10 min at room temperature. Plates were then rinsed with water and air-dried at room temperature overnight. Coloured spots were quantified using an Immunospot S6 Entry Analyzer (Cellular Technology Limited). The splenocytes from each animal were tested in triplicate for each stimulant, except 1V209-TMV (n = 1 per mouse); PMA/ionomycin (n = 1 per mouse); and medium alone (n = 2 per mouse).

Statistical analysis

Data were graphed and analysed by GraphPad Prism v9.0.2. (GraphPad Software). Unless otherwise indicated, comparison was done using one-way analysis of variance (ANOVA) followed by Tukey's multiple comparison test. Significant difference between a study group and control is marked by asterisks and fixed at different statistical levels (*p < 0.05; **p < 0.01; ***p < 0.001; ****p < 0.0001); statistical difference between study groups is marked by hashtags and significance set at different levels (# p < 0.05; ##p < 0.01; ###p < 0.001).

Results

1V209-TMV-PDA formulation

TMV wild type was extracted from *N. benthamiana* with yields of 1.1 g of particles from 100 g of plant leaves. The prepared TMV particles were conjugated to 1V209 using two bifunctional linkers: propargylamine, which was conjugated to TMV's interior glutamates to impart alkyne handles, and aminooxy-PEG1-azide, which was conjugated to 1V209 to enhance its solubility and convey the azide moiety. The alkyne-labeled TMV particles were finally coupled with azide-functionalized 1V209 using click chemistry; and the resultant 1V209-TMV conjugate was coated with PDA (Fig. 1).

1V209-TMV-PDA particles were characterized by SDS-PAGE, LC-MS, and TEM imaging; immunostimulatory and PTT properties were assessed using a Raw-Blue cell assay and photothermal imaging. SDS-PAGE analysis revealed the presence of the TMV coat protein (CP) band at ~18 kDa in all the samples as expected (Fig. 2A). For the 1V209-TMV and 1V209-TMV-PDA samples, the CP band appeared thicker than the band from TMV wild type; this indicates covalent modification of the CP with 1V209, therefore increasing its molecular weight. The additional band appearing at ~39 kDa is a CP dimer, that we typically observe in chemically modified TMV.[16,20,21] LC-MS analysis was performed to confirm the conjugation of 1V209 to TMV coat protein. The MS spectrum of disassembled 1V209-TMV sample showed two prominent mass peaks at 17,591 and 18,144 Da as well as two trace peaks at ~17,000 and ~18,200 Da (Fig. 2B); the MS spectrum of disassembled TMV wild type showed only a single mass peak at 17591 (Supplementary Fig. S1A). This suggests that the mass of TMV CP shifted to higher values in 1V209-TMV spectrum, indicating successful conjugation because the obtained 18,144 Da corresponds to the calculated mass of the expected 1V209-CP conjugate (18,115 Da) plus the mass of one sodium ion ad six protons. Using the mass to charge ratios corresponding to CP (+ESI EIC 1173) and 1V209-CP conjugate (+ESI EIC 1210), two distinct peaks were found in the chromatogram of the disassembled 1V209-TMV sample at elution times of 11.70 min and 11.77 min, respectively (Supplementary Fig. S1B), and from the peak areas the loading was found to be 25 % or 538 molecules of 1V209 per TMV particle. Lastly, we confirmed the structural integrity of 1V209-TMV and 1V209-TMV-PDA particles by TEM (Fig. 2C). Further, successful coating of 1V209-TMV-PDA was indicated by knot-like bumps surrounding the particles.[20,21]

To assay for immunostimulatory properties, we used RAW-Blue cells, which are murine macrophages that express all TLRs (except TLR5) among other pattern-recognition receptors (PRRs). We demonstrated that the conjugation of 1V209 to TMV conferred prominent immunostimulatory properties as compared to basal control and TMV alone and with negligible differences comparing 1V209-TMV and 1V209-TMV-PDA (Fig. 2D). The temperature profile revealed concentration dependent response to irradiation with an 808 nm NIR laser at 1 W cm^{-2} for 10 min (Fig. 2E), and laser-induced heating capacity of the 0.2 mg mL^{-1} 1V209-TMV-PDA was maintained after several irradiation cycles (Fig. 2F). This observation confirms the presence of the PDA coat and established the photothermal capacity of 1V209-TMV-PDA particles prepared for photothermal immunotherapy.

Photothermal immunotherapy of dermal melanoma

To evaluate the anti-tumor efficacy of 1V209-TMV-PDA, we intradermally implanted B16F10 cells into the right flank of C57BL/6 mice, and melanoma-bearing mice were randomly assigned to one of the following I.T. treatment groups: (i) PBS; (ii) 200 μg 1V209-TMV; (iii) 200 μg 1V209-TMV-PDA; (iv) 200 μg 1V209-TMV-PDA followed by 808 nm NIR laser irradiation of the tumor at 1 W cm^{-2} for 5 min; and (v) laser irradiation only. Treatments were administered when tumor volumes reached ~100 mm^3, which was 10 days post tumor inoculation (Fig. 3A). Tumors in the laser treatment groups were irradiated 2 h post intratumoral injection of 1V209-TMV-PDA and controls. The local temperature at the tumor site was monitored throughout the irradiation period (Supplementary Fig. S2A). Tumors treated with 1V209-TMV-PDA + laser and those treated with laser alone

were no longer visually noticeable 2 days post treatment, while for other groups tumors were obvious and disease progression was evident (Fig. 3B). Data indicate potent tumor ablation – even when using the laser alone. Tumor progression or treatment efficacy was also correlated with body weight; body weight increased more rapidly as tumor progressed (Fig. 3C). This data suggests laser-induced local heating of melanoma even in the absence of a PTT agent (Supplementary Fig. S2B); this is consistent with previous reports[9] and can be explained by light-absorbing melanocytes.[34] We observed local tumor recurrence in laser only and 1V209-TMV-PDA-treated groups, however the rate of recurrence was more profound in the laser only group demonstrating efficacy of the designed TMV-based PTT agent. The increased potency of 1V209-TMV-PDA + laser vs. laser alone was also reflected by increased survival of the 1V209-TMV-PDA treated vs control group: ~60 % (5/9) of the mice treated with 1V209-TMV-PDA + laser survived for 50 days with undefined median survival, while only 20 % (2/10) of mice treated with laser alone survived and their median survival was 25 days (Fig. 3D). This data demonstrates potency of the 1V209-TMV-PDA-assisted PTT approach, which synergistically ablated tumors and inhibited tumor recurrence.

ELISpot assay using splenocytes from treated and control animals were used to verify that the 1V209-TMV-PDA-assisted PTT treatment induced anti-tumor specific immunity, specifically tumor-specific T cells. ELISpot assay demonstrated that, when splenocytes were exposed to the B16F10 cells vs. non-target tumor cells, i.e. CT26, or healthy fibroblasts, i.e. NIH3T3 cells, splenocytes from mice treated with 1V209-TMV-PDA + laser produced significantly greater IFN-γ spot-forming cells (SFC) than splenocytes from mice treated with laser only (which in turn outperformed the control group) (Fig. 4, Supplementary Table S1). This data indicates the establishment of anti-tumor immune memory and highlight the potential of 1V209-TMV-PDA in photothermal immunotherapy. The PDA coating on TMV confers PTT properties and 1V209 provides additional signalling through TLR-7 stimulating and boosting anti-tumor immunity. This anti-tumor potency was not achieved using TMV-PDA PTT (Supplementary Fig. S3A–D), which can be explained by the lack of immunostimulatory properties of TMV alone (see Fig. 2D).

Discussion

PTT has shown to be a promising anticancer treatment that remediates local tumors and stimulates the immune system through heat-mediated immunogenic cell death.[35] Nonetheless, numerous studies demonstrated that PTT-induced immunity is ineffective in combating recurrence and metastatic outgrowth, and that the combination with small molecule or nanoparticles-based immunotherapies was necessary for optimal outcome.[36,37] This study highlights the potential of TMV nanoparticles as a platform technology that can accommodate both a PTT agent and an immunotherapeutic booster in a single dosage form. This is an additional asset given that VNPs in general, unlike synthetic nanoparticles, already offer the advantage of easy production of high-quality nanoparticles with excellent homogeneity, reproducibility, and affordability.[38] TMV, in particular, offers the advantage of structure rigidity as well as the possibility for multifaceted (interior and exterior) functionalization with multivalency, which can accommodate co-loading of several cargoes irrespective of their nature (including immunogenic molecules).[39] In this study, by labeling TMV interior glutamates at positions 97 and 106 with propargylamine, we set out to

covalently load the azide-labeled TLR7 agonist 1V209 on TMV using click chemistry; pre-labeling of 1V209 in 50 % DMSO with PEGylated azide was necessary for improved drug solubility to ensure successful bioconjugation under mild condition (i.e., 10 % DMSO). Successful synthesis of the 1V209-TMV conjugate was determined using SDS-PAGE, and further confirmed by LC-MS analysis. The synthesized 1V209-TMV particles were further modified on the surface through PDA coating, which was confirmed by characterizing the microscopic and photothermal features pertaining to the PDA coat. The immunogenic potency of the formulated nanoparticles was initially determined in vitro through TLR7 stimulation in RAW-Blue™ cells; we found that both PDA-coated and uncoated 1V209-TMV particles were effective in RAW-Blue™ cells signalling, suggesting PDA does not interfere with the immunogenicity of other formulation components. While non irradiated mice showed similar disease burden as the untreated PBS group, we found no visible tumors two days following laser irradiation (with or without 1V209-TMV-PDA injection). The limitation of laser treatment alone as a monotherapy was evident; while 60 % mice treated with 1V209-TMV-PDA + laser showed much longer survival, with the median survival beyond 50 days (undefined), the surviving 20 % of mice treated with laser alone showed a median survival of 25 days. Given the fact that we only tested a single treatment dose, the observed preclinical efficacy is highly promising because it appears to be on par with the clinical efficacy of 2–3 cycles of other photo-immunotherapies using indocyanine green as photothermal agent: in one study, PTT combined with imiquimod was effective in 6/11 melanoma patients (with 12-month survival of 70 %);[40] in another study, PTT combined with glycated chitosan as immunoadjuvant showed partial responses in 4/10 breast cancer patients and only 1/10 patients was completely healed over 12 weeks.[41]

Albeit our study primarily aimed at assessing combine PTT-immunotherapeutic efficacy, we set out to verify the benefits of combining 1V209-TMV-PDA with laser (instead of laser only) by assessing immune memory through splenocyte activation in the presence of tumor cells (using ELISpot). It is well stablished that cytotoxic CD8+ T lymphocytes (CTLs) are among the most effective killer cells and are therefore the most approachable aim for cancer immunotherapy.[42] The activation of CTLs mostly relies on antigen presenting cells (APCs; e.g. macrophages and dendritic cells (DCs)), which cross-present tumor-associated antigens (TAAs) to naïve T cells.[43] The effectiveness of this cross-presentation depends on the activation of DCs in tumor tissue, where activated DCs can release chemokines for T cell recruitment eliciting the anti-tumor effect.[44] However, a tumor suppressive microenvironment maintains DCs under an immune suppressive phenotype for the lack of stimulators to PRRs (e.g. TLR7) in DCs. Building on this, the PRR-targeted agonist such as 1V209 to TLR7 might be used to converse the immunosuppressive state of DCs and successfully elicit an anti-tumor T cell response.[45,46]

To gain insights into the mechanism of anti-tumor efficacy of 1V209-TMV-PDA + laser, we evaluated the activation of splenocytes as the presence of IFN-γ SFCs after re-challenge. IFN-γ is a pleiotropic cytokine causing potent anti-tumor immune responses through several mechanisms such cytostatic, proapoptotic and antiproliferative activities;[47] but it also indicates the presence of memory T cells that become activated after re-exposure to their respective antigen, in this case TAAs from B16F10 cells. For this challenge co-culture with B16F10 cells, we observed a significant enhancement in secretion of IFN-γ by splenocytes

from mice treated with 1V209-TMV-PDA + laser and with laser alone, but no reaction was observed with the other cells lines used (see Fig. 4). There was a 2-fold enhancement in IFN-γ secretion comparing 1V209-TMV-PDA + laser vs. laser alone (313 IFN-γ SFCs vs 163 IFN-γ SFCs ($p = 0.0003$), respectively). This is evidence of established anti-tumor immunity underlaying the superior efficacy of the PTT-immunotherapeutic combination over laser or PTT monotherapy. As expected, splenocytes from naïve mice did not respond to challenge co-culture with neither cancer cell lines nor 1V209-TMV, demonstrating that the priming of T cells is required to trigger the presence of IFN-γ SFCs. While further intensive immunotherapeutic studies are underway in our labs, the present findings already highlight the potential of TMV nanoparticles to serve as a multifunctional template for the translational development of one-for-all anticancer photothermal immunotherapy.

Supplementary Material

Refer to Web version on PubMed Central for supplementary material.

Acknowledgements

References

1. American Cancer Society. Melanoma skin cancer. Https://Www.Cancer.Org/Cancer/Melanoma-Skin-Cancer/about/Key-Statistics.Html 2022.

2. Huang S, Zhang Y, Wang L, Liu W, Xiao L, Lin Q, et al. Improved melanoma suppression with target-delivered TRAIL and paclitaxel by a multifunctional nanocarrier. J Control Release 2020;325:10–24, 10.1016/j.jconrel.2020.03.049. [PubMed: 32251770]

3. Rasmussen LA, Jensen H, Virgilsen LF, Rosenkrantz L, Hölmich, Vedsted P A validated register-based algorithm to identify patients diagnosed with recurrence of malignant melanoma in Denmark. Clin Epidemiol 2021;13:207–14, 10.2147/CLEP.S295844. [PubMed: 33758549]

4. Chen Q, Hu Q, Dukhovlinova E, Chen G, Ahn S, Wang C, et al. Photothermal therapy promotes tumor infiltration and antitumor activity of CAR T cells. Adv Mater 2019;31(23):1–7, 10.1002/adma.201900192.

5. Celine Hernandez, Peter Huebener, Schwabe FR Damage-associated molecular patterns in cancer: a double- edged sword. Oncogene 2016;35 (46):5931–41, 10.1038/onc.2016.104.Damage-associated. [PubMed: 27086930]

6. Sweeney EE, Cano-Mejia J, Fernandes R. Photothermal therapy generates a thermal window of immunogenic cell death in neuroblastoma. Small 2018;14(1800678), 10.1002/smll.201800678.

7. Bear AS, Kennedy LC, Young JK, Perna SK, Mattos Almeida JP, Lin AY, et al. Elimination of metastatic melanoma using gold nanoshell-enabled photothermal therapy and adoptive T cell transfer. PLoS One 2013;8(7)e69073, 10.1371/journal.pone.0069073. [PubMed: 23935927]

8. Li Y, Li X, Zhou F, Doughty A, Hoover AR, Nordquist RE, et al .Nanotechnology-based photoimmunological therapies for cancer. Cancer Lett 2019;442:429–38, 10.1016/j.canlet.2018.10.044. [PubMed: 30476523]

9. Chen W, Qin M, Chen X, Wang Q, Zhang Z, Sun X. Combining photothermal therapy and immunotherapy against melanoma by poly-dopamine-coated Al 2 O 3 nanoparticles. Theranostics 2018;8(8): 2229–41, 10.7150/thno.24073. [PubMed: 29721075]

10. Shahrivarkevishahi A, Luzuriaga MA, Herbert FC, Tumac AC, Brohlin OR, Wijesundara YH, et al. PhotothermalPhage: a virus-based photo-thermal therapeutic agent. J Am Chem Soc 2021;143(40):16428–38, 10.1021/jacs.1c05090. [PubMed: 34551259]

11. Mao C, Beiss V, Fields J, Steinmetz NF, Fiering S. Cowpea mosaic virus stimulates antitumor immunity through recognition by multiple MYD88-dependent toll-like receptors. Biomaterials 2022;275(120914), 10.1016/j.biomaterials.2021.120914.Cowpea.

12. Lizotte PH, Wen AM, Sheen MR, Fields J, Rojanasopondist P, Steinmetz NF, et al. In situ vaccination with cowpea mosaic virus nanoparticles suppresses metastatic cancer. Nat Nanotechnol 2016;11(3): 295–303, 10.1038/nnano.2015.292. [PubMed: 26689376]

13. Shoeb E, Badar U, Venkataraman S, Hefferon K. Frontiers in bioengineering and biotechnology: plant nanoparticles for anti-cancer therapy. Vaccines 2021;9(830), 10.3390/vaccines9080830.

14. Shoeb E, Hefferon K. Future of cancer immunotherapy using plant virus-based nanoparticles. FuturSciOA 2019;5(7)FSO401.

15. Venkataraman S, Apka P, Shoeb E, Badar U, Hefferon K. Plant virus nanoparticles for anti-cancer therapy. Front Bioeng Biotechnol 2021;9 (642794), 10.3389/fbioe.2021.642794. [PubMed: 34976959]

16. Wu Z, Zhou J, Nkanga CI, Jin Z, He T, Borum RM, et al. One-step supramolecular multifunctional coating on plant virus nanoparticles for bioimaging and therapeutic applications. ACS Appl Mater Interfaces 2022;14(11):13692–702, 10.1021/acsami.1c22690. [PubMed: 35258299]

17. Bruckman MA, Randolph LN, Gulati NM, Stewart PL, Steinmetz NF. Silica-coated Gd(DOTA)-loaded protein nanoparticles enable magnetic resonance imaging of macrophages. J Mater Chem B 2015;3(38):7503–10, 10.1039/c5tb01014d. [PubMed: 26659591]

18. Gulati NM, Pitek AS, Czapar AE, Stewart PL, Steinmetz NF. Thein vivo fates of plant viral nanoparticles camouflaged using self-proteins: overcoming immune recognition. J Mater Chem B 2018;6(15):2204–16, 10.1039/c7tb03106h. [PubMed: 30294445]

19. Schlick TL, Ding Z, Kovacs EW, Francis MB. Dual-surface modification of the tobacco mosaic virus. J Am Chem Soc 2005;127(11):3718–23, 10.1021/ja046239n. [PubMed: 15771505]

20. Hu H, Yang Q, Baroni S, Yang H, Aime S, Steinmetz NF. Polydopamine-decorated tobacco mosaic virus for photoacoustic/magnetic resonance bimodal imaging and photothermal cancer therapy. Nanoscale 2019;11 (19):9760–8, 10.1039/c9nr02065a. [PubMed: 31066418]

21. Nkanga CI, Chung YH, Shukla S, Zhou J, Jokerst JV, Steinmetz NF. Thein vivo fate of tobacco mosaic virus nanoparticle theranostic agents modified by the addition of a polydopamine coat. Biomater Sci 2021;9 (21):7134–50, 10.1039/d1bm01113h. [PubMed: 34591046]

22. Nam J, Son S, Ochyl LJ, Kuai R, Schwendeman A, Moon JJ. Chemophotothermal therapy combination elicits anti-tumor immunity against advanced metastatic cancer. Nat Commun 2018;9(1074), 10.1038/s41467-018-03473-9.

23. Li M, Guo R, Wei J, Deng M, Li J, Tao Y, et al. Polydopamine-based nanoplatform for photothermal ablation with long-term immune activation against melanoma and its recurrence. Acta Biomater 2021;136(17): 546–57, 10.1016/j.actbio.2021.09.014. [PubMed: 34536603]

24. Seth A, Gholami Derami H, Gupta P, Wang Z, Rathi P, Gupta R, et al. .Polydopamine-mesoporous silica core-shell nanoparticles for combined photothermal immunotherapy. ACS Appl Mater Interfaces 2020;12(38): 42499–510, 10.1021/acsami.0c10781. [PubMed: 32838525]

25. Murray AA, Wang C, Fiering S, Steinmetz NF. In situ vaccination with cowpea vs tobacco mosaic virus against melanoma. Mol Phar 2018;15(9):3700–16, 10.1021/acs.molpharmaceut.8b00316.

26. Chi H, Li C, Zhao FS, Zhang L, Ng TB, Jin G, et al. Anti-tumor activity of toll-like receptor 7 agonists. Front Pharmacol 2017;8(304):1–10, 10.3389/fphar.2017.00304. [PubMed: 28149278]

27. Smits ELJM, Ponsaerts P, Berneman ZN, Tendeloo VFI. The use ofTLR7 and TLR8 ligands for the enhancement of cancer immunotherapy. Oncologist 2008;13(8):859–75, 10.1634/theoncologist.2008-0097. [PubMed: 18701762]

28. Hayashi T, Chan M, Norton JT, Wu CCN, Yao S, Cottam HB, et al. Additive melanoma suppression with intralesional phospholipid-conjugated TLR7 agonists and systemic IL-2. Melanoma Res 2011;21(1):66–75, 10.1097/CMR.0b013e328340ce6c. [PubMed: 21030882]

29. Battistella C, Callmann CE, Thompson MP, Yao S, Yeldandi AV, Hayashi T, et al. Delivery of immunotherapeutic nanoparticles to tumors via enzyme-directed assembly. Adv Healthc Mater 2019;8(23):5–9, 10.1002/adhm.201901105.

30. Shinchi H, Crain B, Yao S, Chan M, Zhang SS, Ahmadiiveli A, et al. Enhancement of the immunostimulatory activity of a TLR7 ligand by conjugation to polysaccharides. Bioconjug Chem 2015;26(8):1713–23, 10.1021/acs.bioconjchem.5b00285. [PubMed: 26193334]

31. Chan M, Hayashi T, Kuy CS, Gray CS, Wu CCN, Corr M, et al. Synthesis and immunological characterization of toll-like receptor 7 agonistic conjugates. Bioconjug Chem 2009;20(6):1194–200, 10.1021/bc900054q. [PubMed: 19445505]

32. Bruckman MA, Steinmetz NF. Chemical modification of the inner and outer surfaces of tobacco mosaic virus (TMV). In: Lin B, Ratna B, editors. Virus Hybrids as Nanomater. Methods Protoc. Totowa, NJ: Humana Press; 2020. p. 173–85, 10.7551/mitpress/12605.003.0016.

33. Hu H, Zhang Y, Shukla S, Gu Y, Yu X, Steinmetz NF. Dysprosium-modified tobacco mosaic virus nanoparticles for ultra-high-field magnetic resonance and near-infrared fluorescence imaging of prostate cancer. ACS Nano 2017;11(9):9249–58, 10.1021/acsnano.7b04472. [PubMed: 28858475]

34. Colombo LL, Vanzulli SI, Blázquez-Castro A, Terrero CS, Stockert JC. Photothermal effect by 808-nm laser irradiation of melanin: a proof-of-concept study of photothermal therapy using B16–F10 melanotic melanoma growing in BALB/c mice. Biomed Opt Express 2019;10(6):2932, 10.1364/boe.10.002932. [PubMed: 31259063]

35. Tian Y, Younis MR, Tang Y, Liao X, He G, Wang S, et al. Dye-loaded mesoporous polydopamine nanoparticles for multimodal tumor theranostics with enhanced immunogenic cell death. JNanobiotechnol 2021; 19(365):1–16, 10.1186/s12951-021-01109-7.

36. Xu P, Liang F. Nanomaterial-based tumor photothermal immunotherapy. Int J Nanomedicine 2020;15:9159–80, 10.2147/IJN.S249252. [PubMed: 33244232]

37. Sun Y, Feng X, Wan C, Lovell JF, Jin H, Ding J. Role of nanoparticle-mediated immunogenic cell death in cancer immunotherapy. Asian JPharm Sci 2020;16(2):129–32, 10.1016/j.ajps.2020.05.004. [PubMed: 33995609]

38. Chung YH, Cai H, Steinmetz NF. Viral nanoparticles for drug delivery, imaging, immunotherapy, and theranostic applications. Adv Drug Deliv Rev 2020;156:214–35, 10.1016/j.addr.2020.06.024. [PubMed: 32603813]

39. Zhao X, Chen L, Luckanagul JA, Zhang X, Lin Y, Wang Q. Enhancing antibody response against small molecular hapten with tobacco mosaic virus as a polyvalent carrier. ChemBioChem 2015;16(9):1279–83, 10.1002/cbic.201500028. [PubMed: 25914312]

40. Li X, Naylor MF, Le H, Nordquist RE, Teague TK, Howard CA, et al. Clinical effects of in situ photoimmunotherapy on late-stage melanoma patients: a preliminary study. Cancer Biol Ther 2010;10(11):1081–7, 10.4161/cbt.10.11.13434. [PubMed: 20890121]

41. Li X, Ferrel GL, Guerra MC, Hode T, Lunn JA, Adalsteinsson O, et al. Preliminary safety and efficacy results of laser immunotherapy for the treatment of metastatic breast cancer patients. Photochem Photobiol Sci 2011;10(5):817–21, 10.1039/c0pp00306a. [PubMed: 21373701]

42. Tan S, Li D, Zhu X. Cancer immunotherapy: pros, cons and beyond. Biomed Pharmacother November 2019;2020:124, 10.1016/j.biopha.2020.109821.

43. Farhood B, Najafi M, Mortezaee K. CD8+ cytotoxic T lymphocytes in cancer immunotherapy: a review. J Cell Physiol 2019;234(6):8509–21, 10.1002/jcp.27782. [PubMed: 30520029]

44. Palucka K, Banchereau J. Cancer immunotherapy via dendritic cells. Nat Rev Cancer 2012;12(4):265–77, 10.1038/nrc3258. [PubMed: 22437871]

45. Marabelle A, Tselikas L, de Baere T, Houot R. Intratumoral immunotherapy: using the tumor as the remedy. Ann Oncol 2017;28(January): xii33–43, 10.1093/annonc/mdx683. [PubMed: 29253115]

46. Mao C, Beiss V, Fields J, Steinmetz NF, Fiering S. Cowpea mosaic virus stimulates antitumor immunity through recognition by multiple MYD88-dependent toll-like receptors. Biomaterials 2021;275(January)120914, 10.1016/j.biomaterials.2021.120914. [PubMed: 34126409]

47. Jorgovanovic D, Song M, Wang L, Zhang Y. Roles of IFN-Γin tumor progression and regression: a review. BiomarkRes 2020;8(49):1–16, 10.1186/s40364-020-00228-x.
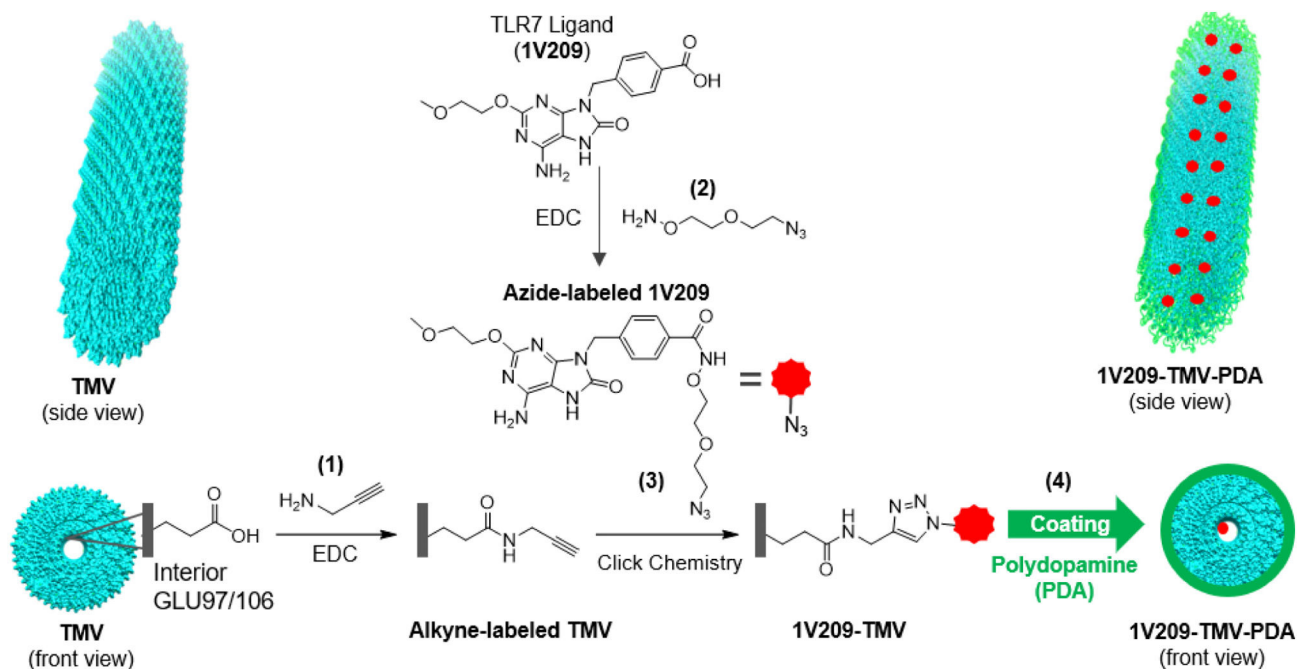
Fig. 1.
Schematic of bioconjugation and coating reactions: (1) alkyne labeling of TMV through EDC-catalyzed amidation of TMV's interior glutamate residues with propargyl amine; (2) azide labeling of 1V209 through EDC-catalyzed amidation of carboxylic group with aminooxy-PEG1-azide; (3) copper-mediated azide–alkyne cycloaddition (CuAAC) producing 1V209-TMV; and (4) polydopamine coating of the prepared 1V209-TMV conjugate using oxidative polymerization of dopamine in alkaline medium (Tris buffer, pH 8.5).
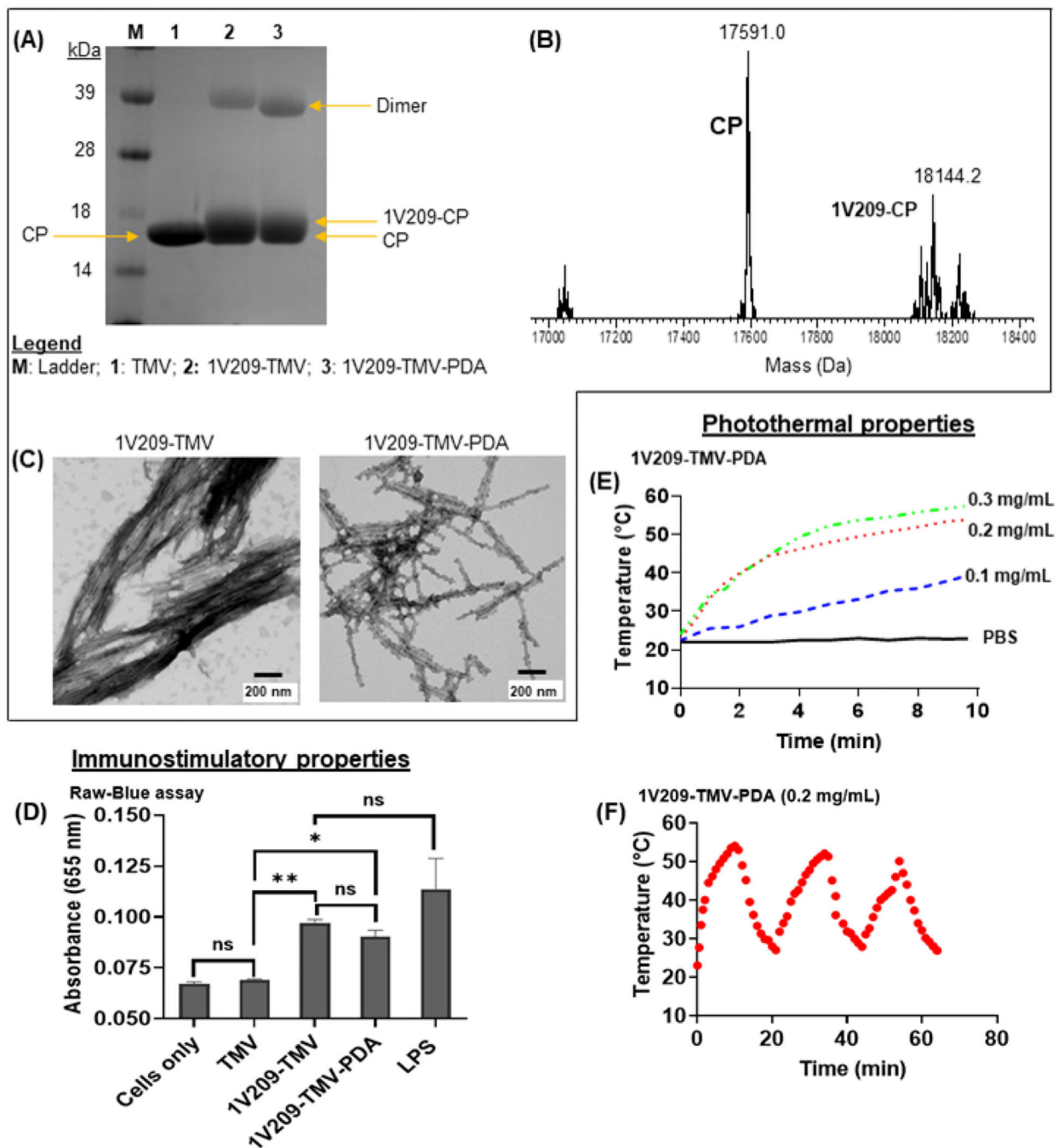
Fig. 2.

Characterization of 1V209-TMV-PDA and their photothermal and immunostimulatory properties: (A) SDS-PAGE gel; the samples in each lane are listed in the legend within the figure panel; (B) ESI-TOFMS spectrum of disassembled 1V209-TMV subunits; (C) TEM micrographs of particles before (1V209-TMV) and after PDA coating (1V209-TMV-PDA); (D) Stimulation of TLR7 in RAW-Blue cells (n = 3). Asterisks indicate significant difference between a given group and the cells only (control) (*p < 0.05; **p < 0.01); ns = not significant. (E) The heating profile of 1V209-TMV-PDA solutions during irradiation with an

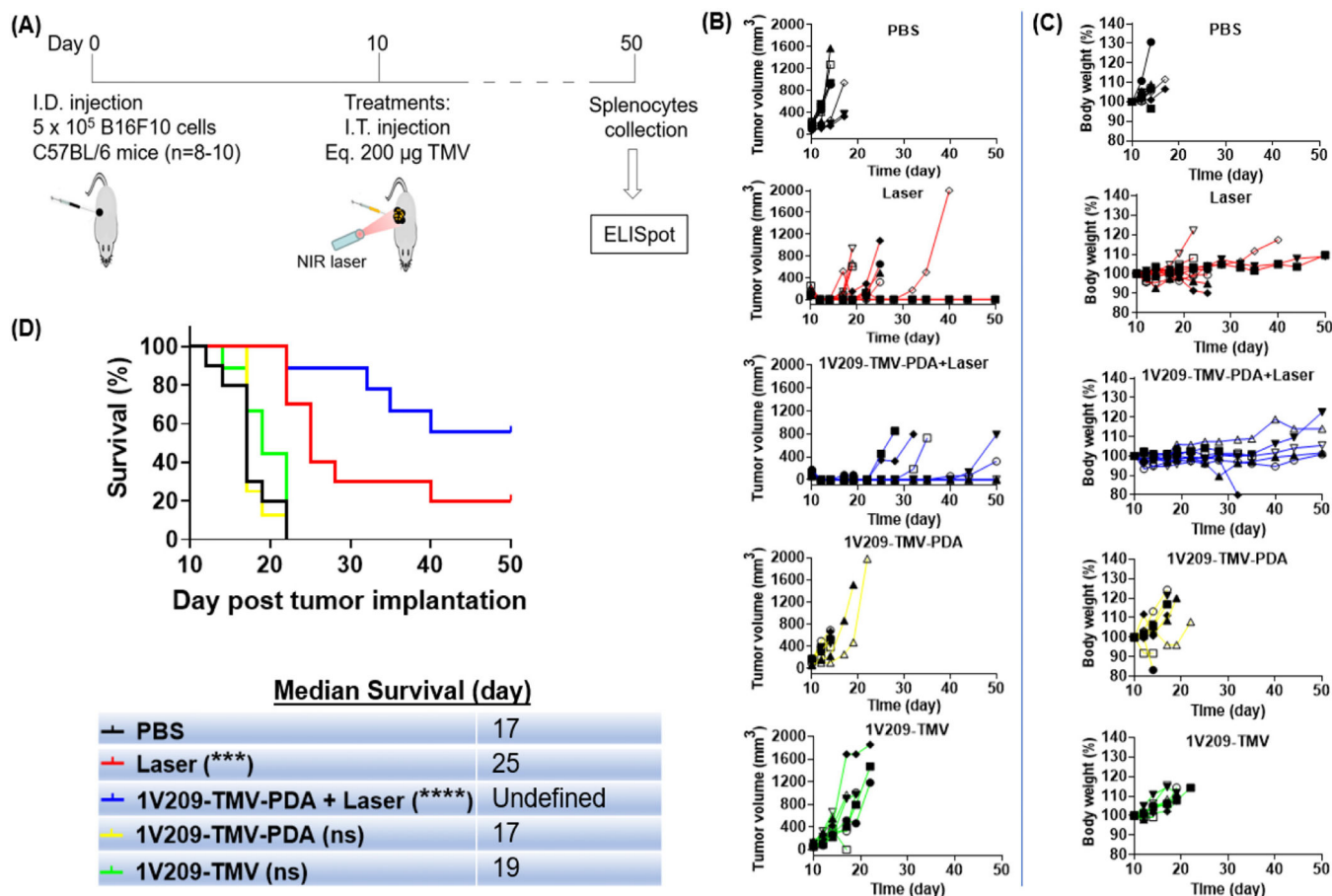808 nm laser at 1 W cm^{-2}; (F) Temperature profile of 0.2 mg mL^{-1} 1V209-TMV-PDA over 3 cycles of 10 min laser on and off.

Fig. 3.
(A) Schematic illustration of TMV-based PTT treatment of melanoma-bearing mice. C57BL/6 mice were intradermally inoculated with B16F10 cells, and ten days later one of the following I.T treatments: PBS (n = 10); 200 μg 1V209-TMV (n = 9); 200 μg 1V209-TMV-PDA only (n = 8); 200 μg 1V209-TMV-PDA followed by 808 nm NIR laser irradiation for 5 min at 1 W cm^{-2}(n = 9) 2 h post injection; and laser irradiation only (n = 10). Individual tumor volume (B) and body weight (C) were measured to assess tumor growth and treatments efficacy. (D) Survival data indicating the trend in disease burden; with PTT showing greater efficacy when combined with immunostimulatory nanoparticles (1V209-TMV-PDA): indicating that 1V209-TMV-PDA + laser irradiation outperformed all other treatment groups (with 50% mice showing median survival 50 days); on day 50 there were 5/9 mice alive in the group of 1V209-TMV-PDA + laser, while in the laser only group there were 2/10 mice alive. Inset the median survival data. Asterisks indicate significant difference between a given group and PBS (control) (***p < 0.001; ****p < 0.0001); ns = not significant.
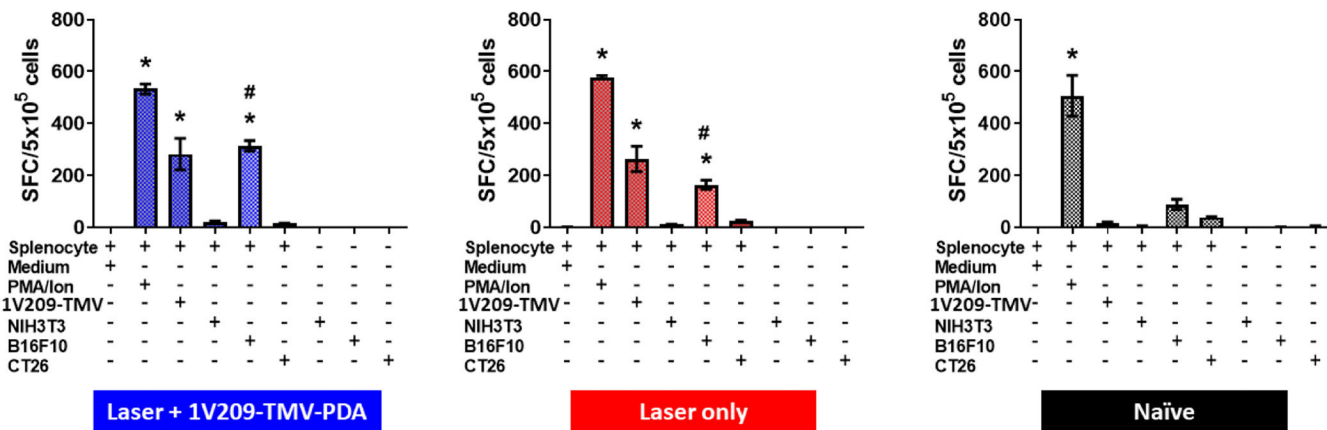
Fig. 4.

Anti-tumor immune memory induced by 1V209-TMV-PDA photothermal immunotherapy. B16F10 cells were I.D. inoculated on day 0; particles were I.T. injected on day 10 and laser irradiation was done 2 h post injections; spleens were harvested on day 50 post tumor inoculation (day 40 post treatment), mice were euthanized, splenocytes were harvested and co-cultured with B16F10, CT26, and NIH3T3 cells for 36 h. Data indicating significant increment of IFN-γ spot-forming cells (SFC) by splenocytes from mice treated with 1V209-TMV-PDA + laser irradiation (n = 5) vs. mice treated with laser only (n = 2) and the control naïve mice (n = 2). One-way ANOVA followed by Dunnett's post-test: *$p < 0.0001$ vs medium; #$p = 0.0003$ for the difference in splenocytes response to incubation with B16F10 between laser +1V209-TMV-PDA group versus laser irradiation only (there was 2-fold increase in SFC specific IFN-γ from laser + 1V209-TMV-PDA compared to Laser group).